Comp. Meth. Civil Eng., Vol.4 No.1 (2013) 103 -117

CMCE
Computational Methods in Civil Engineering

Nonlinear inelastic static analysis of plane frames with numerically generated tangent stiffness matrices

R. Khajavi*

Earthquake Research Center, Ferdowsi University of Mashhad, Iran

Received 10 March 2014; accepted in revised form 4 July 2014

Abstract

For the nonlinear analysis of structures using the well known Newton-Raphson Method, the tangent stiffness matrices of the elements must be constructed in each iteration. Due to the high expense required to find the exact tangent stiffness matrices, researchers have developed novel innovations into the Newton-Raphson method to reduce the cost and time required by the analysis. In this paper, a new approach is suggested to generate the tangent stiffness matrix numerically from internal forces for the materially nonlinear analysis of structures. The method is organized at the element level and, as is verified by numerical experiments, affords good stability and preserves the convergence rate near that of the original exact Newton-Raphson version. To implement the method, an appropriate configuration is first sought for the stiffness matrix of the finite element, which satisfies the element equilibrium requirement; then, the entries of this matrix template are generated from the generalized internal forces of the element by the numerical method of finite differences. The method is applied to construct the stiffness matrix of the plane frame element, which will be used in the analysis of some sample frame structures with materially nonlinear behavior, under monotonic static loading.

Keywords: Finite element, Plane Frame, Nonlinear analysis, Numerical stiffness matrix.

1. Introduction

Nonlinear inelastic analysis becomes inevitable when engineering structures go beyond the elastic range due to the large loads of an earthquake or blast. To maintain the simplicity of structural design procedures, provisions such as FEMA-356 [1] and ATC-40 [2] recommend nonlinear static procedures (NSP) rather than dynamic procedures. Nonlinear static analysis, which considers structural behavior beyond the elastic domain, provides some useful information that cannot be obtained by linear static or dynamic procedures [3].

The iterative Newton-Raphson method is a key tool for solving nonlinear systems of equations in structural engineering. The method has the advantage of a quadratic asymptotic

* Corresponding author.
E-mail address: rezakhajavi@ferdowsi.um.ac.ir

rate of convergence, but is generally considered to be an expensive and time-consuming process [4] as the tangent stiffness matrices for all elements must be obtained through computationally-expensive integration procedures. The process appears to be more costly as the constitutive relations get more complexes.

Several different innovations have been developed to reduce the computational expense of the Newton-Raphson method [5]. Some approaches are based on approximating the tangent stiffness matrix, which may be more efficient than computing it exactly. Application of these methods, though may cause a decrease in the convergence rate, will improve the iterative algorithm, as a consequence of less computational effort.

Methods that incorporate estimates of the tangent stiffness matrix have not yet been used for the inelastic analysis of frame structures. In all of the various approaches adopted for this kind of analysis, from lumped and spread plasticity to inelastic fiber procedures, several methods are proposed to update the exact tangent stiffness matrix at each iteration. Examples of such methods are available in the literature [6-8].

An exact evaluation for the tangent stiffness matrix might not be necessary to solve a nonlinear system of equations iteratively, though it ensures the solution at the most rapid convergence rate [4]. In this paper, a new method is proposed to estimate the tangent stiffness matrix of a finite element from internal forces, using the numerical method of finite differences. It can be used for materially nonlinear analysis under static monotonic loading. Such a method has already been applied to geometrically nonlinear problems [9]. However, the procedure used here for materially nonlinear structures is different from what has been previously proposed [9] for geometrically nonlinear analysis.

The proposed method is implemented in two steps. In the first step, an appropriate configuration is found for the tangent stiffness matrix of the finite element that satisfies the fundamental equilibrium equations at the element level. This characteristic is necessary to ensure the convergence of the iterations [10]. Once the configuration for the tangent stiffness matrix is obtained, its entries will be generated numerically at the second step. The aim of this research is to implement the method for the plane frame element to be used in the inelastic analysis of plane frame structures under monotonic static loads. Numerical experiments are then presented to verify how the method might follow the exact Newton-Raphson procedure.

2. Generalized stiffness formulation

In the following formulation, displacements are assumed to be small and the equilibrium equations are established for the undeformed state of the finite element as a Lagrangian coordinate system, so the geometrical nonlinearity may be ignored. The constitutive law is supposed to be nonlinear, while the kinematic relations are assumed to be linear. Moreover, the relations that follow are all established at the element level.

An inelastic structure under a monotonic static load follows a nonlinear equilibrium path, rather than a linear one. The elements making up the structure also have this property. For each element, the equilibrium equations may be written as

$$\boldsymbol{f}_{D\,int}(\boldsymbol{u}_D) = \boldsymbol{f}_{Dext} \tag{1}$$

where $\boldsymbol{f}_{Dext}$ is the external nodal force vector exerted on the element, while $\boldsymbol{f}_{Dint}$ is the internal nodal force vector of the element, which is a function of the element's nodal displacements $\boldsymbol{u}_D$. This vector can be obtained from the nodal displacements of the structure when the equilibrium equations are being solved at the structure level.

There is no direct method to solve the nonlinear equilibrium equations in the structural analysis; rather, incremental-iterative solution algorithms are mostly employed. These algorithms deal with the nonlinear problem by iteratively solving a series of incremental linear equations. For the displacement-based formulation, an increment of the nodal displacement vector is obtained at each iteration. Summing the increments gives the total nodal displacement up to the current iteration. Thus, the nonlinear equilibrium equations (equation 1) can be converted to the following incremental linear equations for each iteration *i* of the given step *n*:

$$\boldsymbol{K}_{\boldsymbol{D}}^{n,i}\ \mathrm{a}\,\boldsymbol{u}_{\boldsymbol{D}}^{n,i} = \mathrm{a}\,\boldsymbol{f}_{\boldsymbol{D}}^{n,i} \tag{2a}$$

$$\boldsymbol{u}_{\boldsymbol{D}}^{n,i} = \boldsymbol{u}_{\boldsymbol{D}}^{n,i\text{-}1} + \mathrm{a}\boldsymbol{u}_{\boldsymbol{D}}^{n,i} \tag{2b}$$

$$\mathrm{a}\,\boldsymbol{f}_{\boldsymbol{D}}^{n,i} = \boldsymbol{f}_{Dext}^{n,i} - \boldsymbol{f}_{\boldsymbol{D}int}^{n,i}(\boldsymbol{u}_{\boldsymbol{D}}^{n,i}) \tag{2c}$$

Here, the residual force vector $\mathrm{a}\,\boldsymbol{f}_{\boldsymbol{D}}^{n,i}$ is defined as the difference between the external force $\boldsymbol{f}_{Dext}^{n,i}$ and the internal force $\boldsymbol{f}_{\boldsymbol{D}int}^{n,i}$, and $\boldsymbol{K}_{\boldsymbol{D}}^{n,i}$ represents the stiffness matrix of the element, which may change at each iteration according to the numerical solution method adopted. For simplicity, the pointers *i* and *n* are omitted henceforth from the equations:

$$\boldsymbol{K}_{\boldsymbol{D}}\ \mathrm{a}\,\boldsymbol{u}_{\boldsymbol{D}} = \mathrm{a}\,\boldsymbol{f}_{\boldsymbol{D}} \tag{3a}$$

$$\mathrm{a}\,\boldsymbol{f}_{\boldsymbol{D}} = \boldsymbol{f}_{Dext} - \boldsymbol{f}_{\boldsymbol{D}int}(\boldsymbol{u}) \tag{3b}$$

From a mathematical point of view, the matrix $\boldsymbol{K}_D$ may be interpreted as a representation for the linear transformation $\mathrm{h}\ :\ \mathrm{a}\boldsymbol{U}^{\boldsymbol{n_e}} \rightarrow \mathrm{a}\boldsymbol{F}^{\boldsymbol{n_e}}$ that maps vectors from the vector space of element displacement increments $\mathrm{a}\boldsymbol{U}^{\boldsymbol{n_e}}$ onto the vector space of residual forces $\mathrm{a}\boldsymbol{F}^{\boldsymbol{n_e}}$. Both spaces have the same dimension, which is equal to the number of degrees of freedom (DOF) n_e of the element. The representation $\boldsymbol{K}_D$ of the linear transformation h is obtained with respect to the standard or canonical basis for the two spaces. The standard basis matrix $\mathrm{c}_{\boldsymbol{D}} = [\boldsymbol{e}_i : 1 \le i \le n_e]$, which is a columnar arrangement of n_e linearly independent standard basic vectors $\boldsymbol{e}_i$, is the identity matrix $\boldsymbol{I}$.

The linear transformation h will have a different representation $\boldsymbol{K}_q$ with respect to another basis, such as $\mathrm{c}_{\boldsymbol{q}} = [¤_{\boldsymbol{q}_i} : 1 \le i \le n_e]$. Denoting by $\boldsymbol{K}_q$ the *generalized stiffness matrix*, the stiffness relation appears in the following new representation with respect to the generalized basis c_q:

$$\boldsymbol{K}_{\boldsymbol{q}}\ \mathrm{a}\,\boldsymbol{u}_{\boldsymbol{q}} = \mathrm{a}\,\boldsymbol{f}_{\boldsymbol{q}} \tag{4a}$$

$$\mathrm{a}\,\boldsymbol{f}_{\boldsymbol{q}} = \boldsymbol{f}_{qext} - \boldsymbol{f}_{\boldsymbol{q}int}(\boldsymbol{u}) \tag{4b}$$

In the above relations, *q* represents the "generalized" indicator. The two representations (3) and (4) of the stiffness relation are inter-related through the following transformations:

$$\boldsymbol{K}_q = \mathrm{c}_q^{\,T} \boldsymbol{K_D} \mathrm{c}_q \tag{5}$$

$$\mathrm{a}\,\boldsymbol{u}_q = \mathrm{c}_q^{\,-T} \mathrm{a}\,\boldsymbol{u_D} \tag{6}$$

$$\mathrm{a}\,\boldsymbol{f}_q = \mathrm{c}_q^{\,T} \mathrm{a}\,\boldsymbol{f_D} \tag{7}$$

where $\mathrm{c}_q{}^T$ denotes the transpose matrix for c_q. Recall that the matrix c_q is invertible, as its columns constitute a set of linear independent vectors.

An appropriate selection of basic vectors may enable the matrix c_q to be decomposed into two partitions:

$$\mathrm{c}_q = [¤_{q_r} : 1 \le r \le n_r \mid ¤_{q_s} : n_r + 1 \le s \le n_s = n_e - n_r] = [\mathrm{c}_{qr} \mid \mathrm{c}_{qs}] \tag{8}$$

The submatrix c_{qr} is a columnar arrangement of the basic vectors for the null space of h, Ker$\mathrm{h}$, which comprises a basis corresponding to n_r element rigid body motions. The other $n_s = n_e - n_r$ basic vectors arrayed in the submatrix c_{qs} represent other strain states modeled by the finite element. As each basic vector $¤_{qr}$ belongs to the null space Ker$\mathrm{h}$, its image under h will be the zero vector in $\mathrm{a}\boldsymbol{F}^{n_e}$. Therefore, each matrix representation of the transformation h, such as $\boldsymbol{K}_D$, when multiplied by $¤_{qr} \in \mathrm{Ker}\,\mathrm{K}$, will give a zero vector in the residual force space:

$$\mathrm{h}_D \mathrm{c}_{qr} = \mathbf{0} \tag{9}$$

Substituting equation 8 into equation 5, we obtain the following block decomposition for the generalized stiffness matrix:

$$\mathrm{h}_q = \begin{bmatrix} \mathrm{h}_{qrr} & \mathrm{h}_{qrs} \\ \mathrm{h}_{qsr} & \mathrm{h}_{qss} \end{bmatrix} \tag{10}$$

The submatrices present in equation 10 may be written as below, by applying equation 9:

$$\mathrm{h}_{qrr} = \mathrm{c}_{qr}^{\,T} \boldsymbol{K_D} \mathrm{c}_{qr} = \mathrm{c}_{qr}^{\,T} (\boldsymbol{K_D} \mathrm{c}_{qr}) = \mathrm{c}_{qr}^{\,T} .\mathbf{0} = \mathbf{0} \tag{11}$$

$$\mathrm{h}_{qrs} = \mathrm{c}_{qr}^{\,T} \boldsymbol{K_D} \mathrm{c}_{qs} = (\mathrm{c}_{qr}^{\,T} \boldsymbol{K_D}) \mathrm{c}_{qs} = (\boldsymbol{K_D} \mathrm{c}_{qr})^T \mathrm{c}_{qs} = \mathbf{0}.\mathrm{c}_{qs} = \mathbf{0} \tag{12}$$

$$\mathrm{h}_{qsr} = \mathrm{c}_{qs}^{\,T} \boldsymbol{K_D} \mathrm{c}_{qr} = \mathrm{c}_{qs}^{\,T} (\boldsymbol{K_D} \mathrm{c}_{qr}) = \mathrm{c}_{qs}^{\,T} .\mathbf{0} = \mathbf{0} \tag{13}$$

$$\mathrm{h}_{qss} = \mathrm{c}_{qs}^{\,T} \boldsymbol{K_D} \mathrm{c}_{qs} \tag{14}$$

These will give the following simplified representation for the generalized stiffness matrix $\boldsymbol{K}_q$ with respect to the basis c_q from equation 8:

$$\mathbf{K}_q = \begin{bmatrix} \mathbf{0}_{n_r \times n_r} & \mathbf{0}_{n_r \times n_s} \\ \mathbf{0}_{n_s \times n_r} & \mathbf{K}_{qss} \end{bmatrix}_{n_e \times n_e} \tag{15}$$

The submatrix $\boldsymbol{K}_{qss}$ is of dimension $n_s \times n_s$, and has a nonzero constant representation when linear elastic behavior is only concerned [11]. For the nonlinear inelastic behavior, however, the submatrix must be refreshed at each iteration. In this case, a singularity condition may occur, or even a non-definite or negative definite matrix may result, depending on the kind of nonlinearity, hardening or softening, that takes place.

Based on the partitioned basis β_q of equation 8, the partitioned stiffness relation is represented as follows:

$$\begin{bmatrix} \mathbf{0} & \mathbf{0} \\ \mathbf{0} & \mathbf{K}_{qss} \end{bmatrix} \begin{Bmatrix} \Delta \boldsymbol{u}_{qr} \\ \Delta \boldsymbol{u}_{qs} \end{Bmatrix} = \begin{Bmatrix} \Delta \boldsymbol{f}_{qr} \\ \Delta \boldsymbol{f}_{qs} \end{Bmatrix} \tag{16}$$

3. Numerically generated tangent stiffness matrix

As discussed before, incremental-iterative solution algorithms are mainly used to solve the nonlinear equilibrium system of equations in structural engineering. The most interested solution procedure is the well known Newton-Raphson method, in which the tangent stiffness matrix is recomputed at each iteration. This enables it to converge at a higher rate than alternatives such as the secant or Newton-like procedures [5, 12].

The tangent stiffness matrix may be considered as the jacobian of the internal force functions: a matrix consisting of the partial derivatives of the nodal internal force functions with respect to the nodal displacements. If the nodal internal force vector $\boldsymbol{f}_{Dint} : \boldsymbol{U}^{n_e} \rightarrow \boldsymbol{F}^{n_e}$ is a function of n_e displacement variables $u_i \in \boldsymbol{U}^{n_e}$,$1 \le i \le n_e$, the tangent stiffness matrix will be:

$$\mathbf{K}_D = \left[\frac{\partial f_{Dint,i}(\boldsymbol{u}_D)}{\partial u_{D,j}} : 1 \le i \le n_e , 1 \le j \le n_e \right] \tag{17}$$

When it is difficult to find the tangent stiffness matrix by the well known finite element formulation or analytical calculation of the jacobian, numerical differentiation algorithms, such as the following forward finite difference method, may be adopted:

$$\mathbf{K}_D = \left[\frac{f_{Dint,i}(u_{D,i} : i \ne j \ , u_{D,j} + \varepsilon \Delta v_{D,j}) - f_{Dint,i}(\boldsymbol{u}_D)}{\varepsilon} : 1 \le i \le n_e , 1 \le j \le n_e \right] \tag{18}$$

where $\Delta \boldsymbol{v}_D = \{\Delta v_{D,j} : 1 \le j \le n_e\}$ is an arbitrary perturbation vector in the space of displacements $\boldsymbol{U}^{n_e}$ with respect to the basis β_D. The scalar number ε is a small constant which may be determined at each iteration according to some known values from the previous iteration. The discretization error for the finite difference method will decrease as the perturbation constant decreases. This will give a more precise assessment for the partial derivative, unless the round-off errors disturb the accuracy of the solution. Therefore, the perturbation constant might have an optimized value. The following numerical expression is used in this research as an estimate for this value [9]:

$$£ = \sqrt{£_{\boldsymbol{m}}} \; . \; \frac{1 + \| \boldsymbol{u}_{\boldsymbol{D}}^{\boldsymbol{n},\boldsymbol{i}-1} \|}{\| \text{a}\boldsymbol{u}_{\boldsymbol{D}}^{\boldsymbol{n},\boldsymbol{i}-1} \|} \tag{19}$$

where $\sqrt{£_{\boldsymbol{m}}}$ is the machine precision, and $\| . \|$ designates the L^2-norm of the vector.

The numerical assessment of the stiffness matrix by equation 18 may suffer two fundamental deficiencies. The first one is nonsymmetry of equation 18, and the second one is its inability to consider a proper number of rigid body motions, RBMs. These deficiencies may hurt the solution accuracy or lead to nonconvergence. To resolve the problem, the stiffness matrix is modified after it is generated numerically, to give it the fundamental features of symmetry and the proper number of RBMs [9].

The tangent stiffness matrix can be rebuilt for the generalized coordinates *q*, as discussed before. The index *D* must then be substituted by *q* in Eqs. 17-19. The following numerical estimate for the generalized tangent stiffness matrix is thus obtained:

$$\text{h}_q = \left[\frac{f_{qint,i}(u_{q,i} : i \neq j \;, u_{q,j} + £ \, \text{a}v_{q,j}) - f_{qint,i}(\boldsymbol{u}_q)}{£} \; : 1 \le i \le n_e \,, 1 \le j \le n_e \right] \tag{20}$$

where $\text{a}\boldsymbol{v}_{\boldsymbol{q}} = \{\text{a}v_{q,j} : 1 \le j \le n_e\}$ is an arbitrary perturbation vector in the space of displacements $\boldsymbol{U}^{n_e}$ with respect to the basis c_q.

4. Numerically generated stiffness matrix for the inelastic frame element

In this section, we describe the numerical generation of the tangent stiffness matrix for the plane two-noded frame element with 6 degrees of freedom. The element has a length *L*, uniform sections with area *A* and area moment of inertia *I*, and inelastic behavior in bending. Nonlinear behavior for axial deformation (tension and compression) is neglected. The nonlinear behavior is indicated by a nonlinear function $M = M(\kappa)$ for each section along the element. The function illustrates how the moment for each section *M* changes with respect to the section curvature © . It may be obtained by experiment or section analysis.

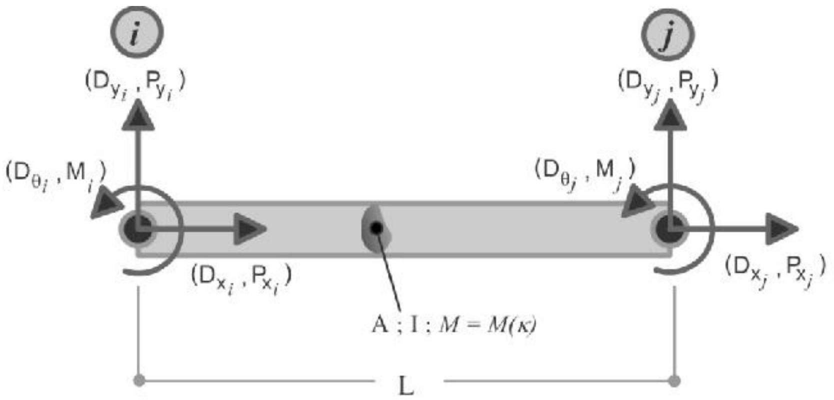

Figure 1. Plane frame element with materially nonlinear behavior

As mentioned before, a key problem in dealing with a numerical stiffness matrix is to maintain a proper number of RBMs. The approach used by Lee and Park [9] for geometrically nonlinear problems is to modify the numerically generated stiffness matrix so that it has the proper rank. However, the present research suggests an inverse procedure for the materially nonlinear problems: first find an appropriate configuration for the stiffness matrix with a proper rank, and then generate the stiffness matrix numerically for the finite element.

Based on the discussion in Section 2, the basic vectors should be categorized into two groups of RBMs and strain states, in order to find an appropriate configuration for the stiffness matrix of the frame element with proper rank. RBMs are those basic deformations that do not store strain energy. The two translational rigid body motions along and perpendicular to the longitudinal axis and the rigid rotation are considered as the three RBMs for the inelastic frame element. The vectors corresponding to these three RBMs constitute a basis for the null space of the inelastic tangent stiffness transformation Ker(h). It is worth noting that the rigid rotation of the frame element stores strain energy in the case of geometrically nonlinear behavior; thus, rigid rotation shall not be considered in the null space of the geometrically nonlinear stiffness transformation [13].

The other three basic vectors selected for the space of element displacement increments $\mathrm{a}\boldsymbol{U}^{n_e}$ represent the strain states that store energy. These vectors, along with the three vectors of RBMs, constitute the six linearly independent basic vectors spanning the space of element displacement increments $\mathrm{a}\boldsymbol{U}^{n_e=6}$. A columnar arrangement of these six vectors will make up the generalized basis matrix c_q:

$$\mathrm{c}_q = [\mathrm{c}_{qr} \,|\, \mathrm{c}_{qs}] = \begin{bmatrix} 1 & 0 & 0 & -L/2 & 0 & 0 \\ 0 & 1 & -L/2 & 0 & L^2/8 & -L^3/48 \\ 0 & 0 & 1 & 0 & -L/2 & L^2/8 \\ 1 & 0 & 0 & L/2 & 0 & 0 \\ 0 & 1 & L/2 & 0 & L^2/8 & L^3/48 \\ 0 & 0 & 1 & 0 & L/2 & L^2/8 \end{bmatrix} \tag{21}$$

Deformations corresponding to these basic displacement vectors are displayed in Figure 2. Ref [11] presents a systematic approach for an appropriate selection of linearly independent basic vectors.

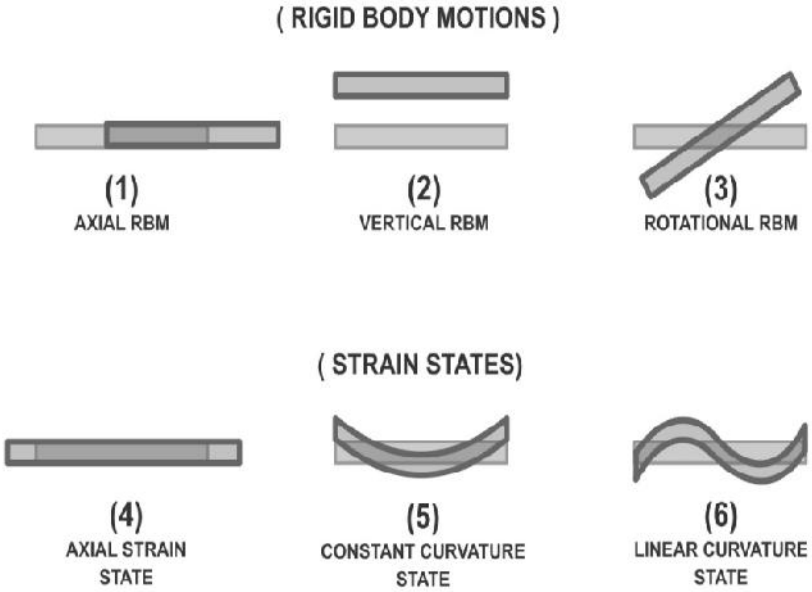

Figure 2. Rigid body motions and strain states for the frame element with materially nonlinear behavior

The stiffness transformation will have the following representation with respect to the basis introduced in equation 21:

$$\mathrm{h}_q = \begin{bmatrix} \mathrm{h}_{qrr} & \mathrm{h}_{qrs} \\ \mathrm{h}_{qsr} & \mathrm{h}_{qss} \end{bmatrix} = \begin{bmatrix} 0 & 0 & 0 & 0 & 0 & 0 \\ 0 & 0 & 0 & 0 & 0 & 0 \\ 0 & 0 & 0 & 0 & 0 & 0 \\ 0 & 0 & 0 & k_{qa} & 0 & 0 \\ 0 & 0 & 0 & 0 & k_{q11} & k_{q12} \\ 0 & 0 & 0 & 0 & k_{q21} & k_{q22} \end{bmatrix} \tag{22}$$

This matrix has a maximum rank of 3, which is the correct maximum rank for the tangent inelastic stiffness matrix. During the analysis procedure, as nonlinear materially-run mechanisms cause the element stiffness to decrease, the rank of the matrix may drop.

In equation 22, k_{qa} represents the generalized axial stiffness corresponding to the axial strain state, and is equal to

$$k_{qa} = EAL \tag{23}$$

where E is the elastic modulus. The entries $\{k_{qij} : i, j = 1,2\}$ in equation 22 comprise the bending stiffness submatrix corresponding to the constant and linear strain states. During the analysis procedure, the generalized axial stiffness k_{qa} remains constant, since by initial assumption, nonlinearity is overlooked for the axial behavior. However, the entries of the bending stiffness submatrix may change during the nonlinear analysis. As is obvious from the submatrix h_{qss}, there is no coupling between the axial and bending deformation components.

This means that no bending strain energy will be stored when the element is subjected to a deformation corresponding to the axial strain state. Deformations pertaining to the bending states also do not trigger axial strain states.

Using equation 20, the entries of the tangent bending stiffness submatrix in equation 22 can be numerically estimated while assuring the proper rank. To do this, it is necessary to find the generalized internal force vector of the frame element. This vector can be obtained from the element nodal internal force vector $f_{D\,int} = \{P_{xi} \quad P_{yi} \quad M_i \quad P_{xj} \quad P_{yj} \quad M_j\}^{\mathrm{T}}$ through a simple transformation:

$$\boldsymbol{f}_{q\,int} = \mathrm{c}_q^T \boldsymbol{f}_{\boldsymbol{D}\,int} \tag{24}$$

equation 24 may be expanded to give the following representation:

$$\begin{Bmatrix} f_{u_{xo}} \\ f_{u_{yo}} \\ f_{\theta_o} \\ f_{qa} \\ f_{q1} \\ f_{q2} \end{Bmatrix} = \begin{Bmatrix} P_{xi} + P_{xj} = 0 \\ P_{yi} + P_{yj} = 0 \\ M_i + M_j + (P_{yj} - P_{yi})\ \mathrm{L}/2 = 0 \\ (P_{xj} - P_{xi}).\ \mathrm{L}/2 \\ (M_j - M_i).\ \mathrm{L}/2 \\ (M_i + M_j).L^2/12 \end{Bmatrix} \tag{25}$$

In the above equation, the generalized internal forces corresponding to the RBMs $f_{u_{xo}}$, $f_{u_{yo}}$ and f_{θ_o} turn out to be zero, as no strain energy is stored in the RBMs. As indicated in equation 25, the zero-valued internal forces corresponding to the RBMs $f_{u_{xo}}$, $f_{u_{yo}}$ and f_{θ_o} pertain to the force equilibrium equations along the two directions x and y, $\sum P_x = 0$ and $\sum P_y = 0$, and the moment equilibrium equation $\sum M = 0$, respectively, all established at the element level. The generalized internal forces, f_{qa}, f_{q1} and f_{q2}, correspond to the axial strain, constant and linear curvature states, respectively. To establish a numerical estimate for the stiffness matrix in equation 22 at iteration *i* of step *n*, f_{q1} and f_{q2} must be determined from the internal moments of all sections along the frame element.

Nodal internal moments are given by the following relation:

$$\begin{Bmatrix} M_i \\ M_j \end{Bmatrix} = \int_0^{\mathrm{L}} [B_3(x) \quad B_6(x)]^T M(\copyright(x))\, dx \tag{26}$$

where B_3 and B_6 represent the third and sixth entries of the displacement-curvature matrix ***B***, respectively, and correspond to the rotational degrees of freedom for the frame element. Based on the Euler-Bernoulli bending theory, the entries of the matrix ***B*** are considered as the second derivatives of the entries for the matrix of shape functions ***N***.

Substituting equation 26 into the two last entries of the vector in equation 25, f_{q1} and f_{q2} are obtained as below:

$$\begin{Bmatrix} f_{q1} \\ f_{q2} \end{Bmatrix} = \begin{Bmatrix} \int_0^{\mathrm{L}} M\, dx \\ \int_0^{\mathrm{L}} (x - L/2) M\, dx \end{Bmatrix} \tag{27}$$

As it is clear from equation 27, f_{q1} equals the algebraic sum of the area under the moment distribution curve along the element. f_{q2} can also be interpreted as the first moment of section moments for the frame element. equation 27 can also be obtained using the generalized displacement-curvature matrix $\boldsymbol{B_q}$. The entries of $\boldsymbol{B_q}$ are second derivatives of the entries in the generalized shape function matrix $\boldsymbol{N_q}$, which can be found from the basic vectors selected in equation 21 [11]. The functions in $\boldsymbol{N_q}$ were already shown in Figure 2.

Using equation 20 and the known relations for f_{q1} and f_{q2}, the entries $\{k_{qij} : i, j = 1,2\}$ for the bending stiffness submatrix can be generated numerically. The method can be summarized as follows: to generate the entry k_{qij}, the basic strain state j is subjected to a small displacement perturbation, causing a nonlinear change in the moment distribution along the frame element. Based on this new moment distribution, the generalized internal forces are calculated from equation 27. The entry k_{qij} can then be obtained from equation 20.

The generalized tangent stiffness matrix generated numerically according to equation 22 may suffer nonsymmetry, though it does turn out to be near-symmetrical, as will be shown by numerical examples in the next section. The symmetry characteristic can be recovered by substituting $\frac{k_{q12} + k_{q21}}{2}$ in place of the non-diagonal entries of the bending stiffness submatrix, k_{q12} and k_{q21}.

The stiffness matrix for the finite element can be obtained from the numerically generated generalized stiffness matrix through the following transformation:

$$\text{h}_D = \text{c}_q^{-T} \boldsymbol{K}_q \text{c}_q \tag{28}$$

It is important to mention that the above transformation might not alter the rank for the transformed matrix, i.e. $rank(\boldsymbol{K}_D) = rank(\boldsymbol{K}_q)$, as c_q is invertible; therefore, the $\boldsymbol{K}_D$ obtained by equation 28 will have the proper rank.

5. Numerical examples

In this section, some numerical experiments are employed to evaluate the proposed method and compare it with its alternatives. For the purpose of simplicity, the input data for the element characteristics are set to unit values.

5.1. Cantilever beam with smooth nonlinear material behavior

A cantilever beam with point load P = 1.1 N at the free end is shown in Figure 3. The beam has uniform cross-section with area A = 1.0 m^2, area moment of inertia I = 1.0 m^4, length L = 1.0 m, Young's modulus E = 1.0 N/m^2, and Poisson's ratio ¬ = 0. The nonlinear behavior of each section along the element is indicated by the explicit nonlinear function $M(x) = EI \frac{©(x)}{1 + L©(x)}$. For a close simulation of the ordinary behavior of steel or reinforced concrete structures, the load P is exerted in such a way that the softening branch, not the hardening one, of the nonlinear function $M = M(©)$ is activated. However, for theoretical consideration, this assumption does not matter.

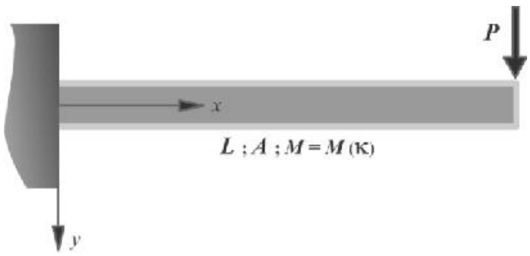

Figure 3. Cantilever beam with tip load

The cantilever beam is modeled by one frame element, and the Newton-Raphson method is used for the analysis, while the tangent stiffness matrix at each iteration is obtained using the following methods:

1. The exact closed-form method (CFSM),
2. equation 18 (the frame element cannot satisfy equation 18, which is a self equilibrium equation)
(NNSM), and
3. The proposed numerical method (NESM).

For all three methods, the integration is performed explicitly.
The results for the nonlinear analysis obtained by the three above methods are illustrated in Figure 4. The perturbation vectors are selected randomly and considered the same for the two numerical methods NNSM and NESM, so that the performance of the methods may be compared appropriately. As is clear from Figure 4, the equilibrium path obtained by the proposed method (NESM) follows the exact path achieved from the closed form relation for the stiffness matrix very closely. However, the analysis obtained from a direct use of equation 18 without satisfying the element equilibrium requirement may not follow the equilibrium path, though at the final point of the increment, it returns close to the exact curve. More studies on this numerical experiment, not presented here, show that the self-equilibrated stiffness matrix obtained by the proposed method is more robust than its non-equilibrated counterpart. The equilibrium path obtained by the proposed method gets small shifts and remains close to the exact equilibrium path when different perturbation vectors are used, while for the non-equilibrated numerical method, large shifts occur, and sometimes the analysis may diverge. The proposed method (NESM) converges in 8 steps, while NNSM converges in 11 steps.

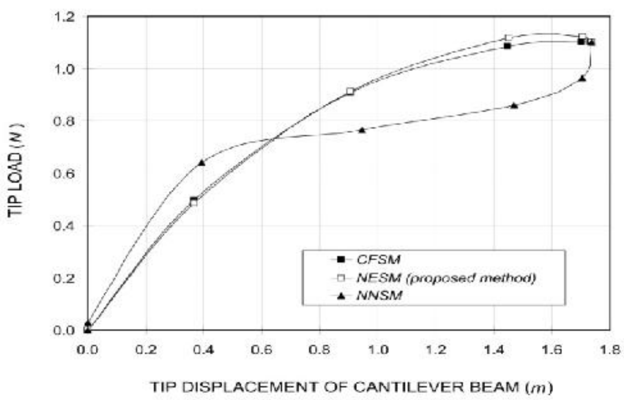

Figure 4. Equilibrium paths obtained by different stiffness matrix generation methods for cantilever beam with smooth nonlinear material behavior

5.2. Cantilever beam with non-smooth nonlinear material behavior

In structural engineering, the nonlinear material behavior of steel or reinforced concrete is mostly modeled by non-smooth multilinear (bilinear or three-linear) curves. In this example, the nonlinear behavior for each section along the element shown in Figure 3 is supposed to be indicated as a three-linear function, shown in Figure 5. The beam characteristics are the same as the previous example. The multilinear function is a well-behaved approximation for the nonlinear sectional behavior function introduced in the previous example.

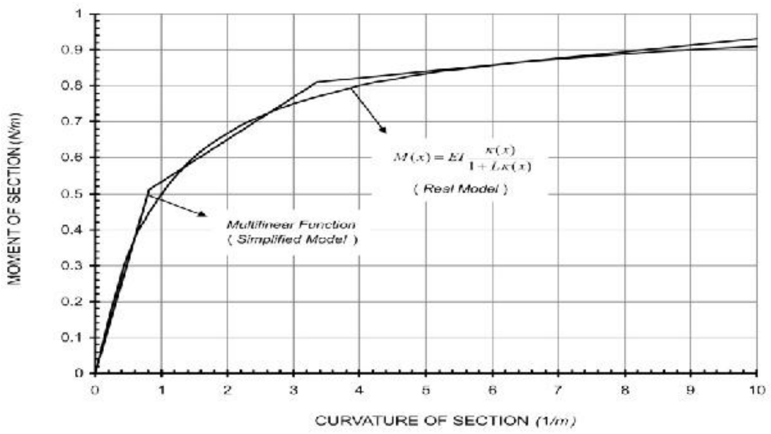

Figure 5. Three-linear simplified model for nonlinear material behavior of the cantilever beam sections

The cantilever beam shown in Figure 3 with nonlinear sectional behavior depicted in Figure 5 is analyzed by the three methods CFSM, NESM and NNSM. A two-point quadrature rule is employed for the integration. As shown in Figure 6, the results obtained by the three methods coincide very closely. Therefore, it may be concluded that the numerical method for tangent stiffness matrix generation performs well when it is applied to multi-linear behavior functions.

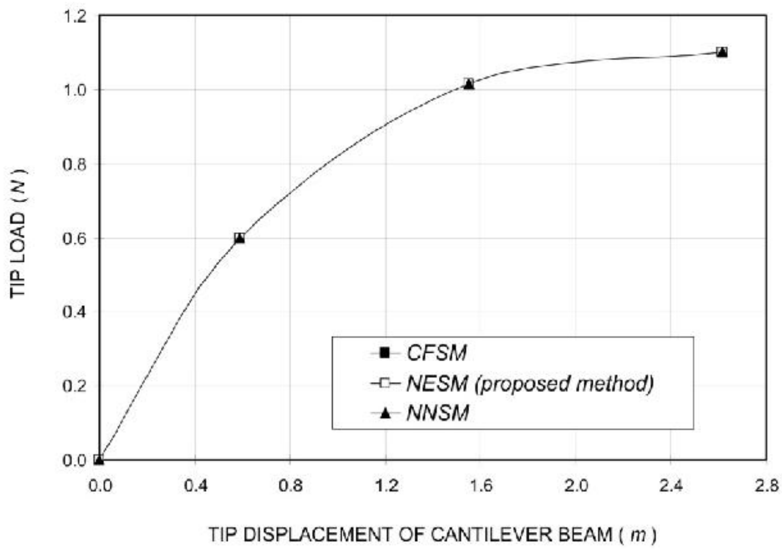

Figure 6. Equilibrium paths obtained by different stiffness matrix generation methods for cantilever beam with three-linear material behavior

5.3. Portal frame with smooth nonlinear material behavior

Consider a portal frame with three elements under lateral loading $P = 4.0$ *N*, as shown in Figure 7. All frame elements have the same uniform sections with area $A = 1.0\ m^2$, area moment of inertia $I = 1.0\ m^4$, and length $L = 1.0\ m$. The nonlinear behavior of the sections is indicated by the nonlinear explicit function $M(x) = \frac{EI}{L} sin(L\ \text{©}(x))$. The function has two smooth softening branches, symmetric with respect to the origin. Geometrical nonlinearity is neglected in the procedure. Each element is modeled by one frame element. The Newton-Raphson method is applied to solve the nonlinear equations of equilibrium, while the tangent stiffness matrices for the elements at each iteration are calculated by the two methods CFSM and NESM.

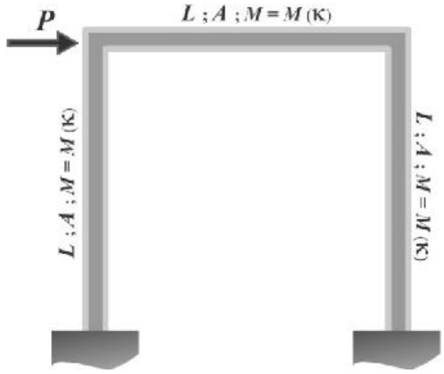

Figure 7. Portal frame with three nonlinear frame elements under lateral loading

The results obtained by the two methods are depicted as lateral load-lateral displacement curves in Figure 8. As the functions appearing in the CFSM method may not be explicitly integrable, a two-point Gauss quadrature rule is employed for integration. However, the tangent stiffness matrices in the NESM method can be explicitly integrated. The discrepancy of results for the two methods turns out to be mostly a consequence of the difference in integration approaches, since the results will approach each other when a two-point Gauss quadrature rule is employed for both methods. It may therefore be concluded that the results obtained by the NESM method and explicit integrating rule are more accurate than the results from CFSM method with approximate integration.

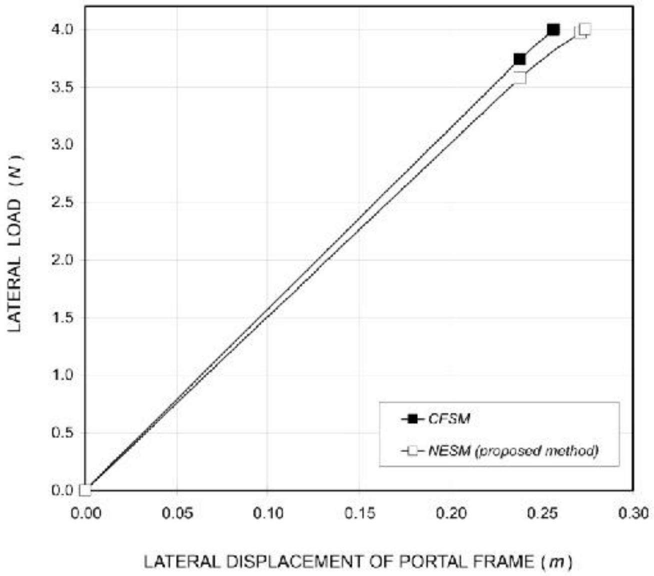

Figure 8. Equilibrium paths obtained by different methods of stiffness matrix generation for portal frame with smooth nonlinear material behavior

6. Conclusion

In this research, a method was proposed to numerically generate the tangent stiffness matrix of the frame element for the analysis of frame structures with nonlinear material behavior. In the first step, a general configuration is recognized to represent the tangent stiffness matrix that maintains the element self-equilibrium requirement by including a proper number of rigid body motion states. The fundamental attribute of the present approach is the decomposition of the basis for the vector space of displacements into the RBMs and stain states. The proposed procedure deals with the tangent stiffness matrix in a generalized coordinate system. In the second step, the entries of the element generalized stiffness matrix are numerically generated for each iteration, using the forward finite difference approximation.

Numerical verification demonstrates some features of the proposed procedure:

1. The proposed procedure is sufficiently accurate. It generates the equilibrium path adequately close to the exact curve. This feature may be interpreted as a consequence of two main points. The first is that the generated tangent stiffness matrix retains the self-equilibrium feature. The second point is the low number of nonzero entries of the generalized stiffness matrix to be numerically evaluated. While in the proposed procedure, only 4 entries must be evaluated to give the stiffness matrix, a 16-entry numerical generation is needed to construct the tangent stiffness matrix for the frame element in other procedures [9]. Moreover, in problems where explicit integration may not be dealt with and an approximate integrating rule has to be employed, numerical generation of the stiffness matrix with exact explicit integration may improve the results; however, this claim requires more investigation and research.
2. The proposed procedure is robust. No considerable shift occurs in the results when the perturbation vector changes. This feature may also be regarded as a consequence of the self-equilibrium characteristic of the frame element, provided in the proposed procedure. Further numerical investigation, not presented in this paper, shows that the numerical procedure that does not satisfy the self-equilibrium requirement suffers a slow convergence rate, low accuracy, and nonconvergence in some cases.
3. The proposed procedure has no limit in its application at the element level. While the numerical method generating the ordinary element stiffness matrix may encounter difficulties due to zero boundary conditions, the proposed method can skip the problem as the stiffness matrix is configured for the generalized coordinates. The problem pertains to the inevitable zero perturbation scalar corresponding to the zero DOF, appearing in the denominator when the finite difference rule is employed. The zero value is substituted by a small number to settle the problem. However, in the proposed method, zero boundary conditions may seldom produce zero-valued coefficients for the strain state basic vectors in practice. Thus, the perturbation scalars might not be zero and the procedure can follow its ordinary regulation.

The present procedure is proposed for the numerical generation of the element stiffness matrix for finite elements with nonlinear constitutive laws, and was implemented for the frame element. The procedure may also be extended to other complex finite elements, including plates and shells. The procedure is fundamentally applicable for structural problems where an exact evaluation for the tangent stiffness matrix is costly or unavailable due to the complex constitutive models.

References

[1] FEMA-356: *Federal Emergency Management Agency*, *Prestandard and commentary for seismic rehabilitation of buildings*, Washington DC, 2000.

[2] ATC-40, *Applied Technology Council*, *Seismic evaluation and retrofit of concrete buildings*, Vols. 1 & 2, California, 1996.

[3] A.M. Mwafy, A.S. Elnashai, Static pushover versus dynamic collapse analysis of RC buildings, *Journal Engineering Structures* 23 (2001) 407–424.

[4] O. C. Zienkiewicz, R. L. Taylor, *Finite Element Method: Solid Mechanics,* vol. 2, Butterworth-Heinemann, London, 2000.

[5] P. Deulflhand, Newton Methods for Nonlinear Problems, *Springer serires in computational mathematics,* Springer-Verlag Berlin Heidelberg, 2004.

[6] F. C. Filippou, A. Issa, Nonlinear static and dynamic analysis of reinforced concrete subassebmblages, Report UCB/EERC–92/08, *Earthquake Engineering Research Center, College of Engineering,* University of California, Berkeley, 1992.

[7] C. Ngo-Huu, S. E. Kim, J. R. Oh, Nonlinear analysis of space steel frames using fiber plastic hinge concept, *Journal Engineering Structures* 29 (2007) 649-657.

[8] H. G. Kwak, S. P. Kim, Nonlinear analysis of RC beams based on moment-curvature relation, *Computers and Structures* 80 (2002) 615-628.

[9] Y. Lee, K. C. Park, Numerically generated tangent stiffness matrices for nonlinear structural analysis, *Computer Methods in Applied Mechanics Engineering* 191 (2002) 5833-5846.

[10] L. J. Leu, Y. B. Yang, Effects of rigid body and stretching on nonlinear analysis of trusses, *ASCE Journal of Structural Engineering* 116 (1990) 2582-2598.

[11] R. Khajavi, Partitioning the stiffness matrix and the principal stiffness matrix of the finite element. MSc Dissertation, Ferdowsi University of Mashhad, Iran, 2004. (in Farsi)

[12] E. Süli, D. Mayers, An Introduction to Numerical Analysis, Cambridge University Press, 2003.

[13] Y. B. Yang, H. T. Chiou, Rigid body motion test for nonlinear analysis with beam elements, *Journal of Engineering Mechanics ASCE* Vol. 113 (1987) 1404-1419.